Development 129, 5255-5268 (2002)
Printed in Great Britain © The Company of Biologists Limited 2002
DEV8935

Roles of the Homothorax/Meis/Prep homolog UNC-62 and the Exd/Pbx homologs CEH-20 and CEH-40 in *C. elegans* embryogenesis

Kimberly Van Auken[1,*], Daniel Weaver[1,†], Barbara Robertson[1], Meera Sundaram[2], Tassa Saldi[1], Lois Edgar[1], Ulrich Elling[1,‡], Monica Lee[1], Queta Boese[1,§] and William B. Wood[1,¶]

[1]Department of Molecular, Cellular and Developmental Biology, University of Colorado, Boulder, CO 80309-0347, USA
[2]Department of Genetics, University of Pennsylvania School of Medicine, Philadelphia, PA 19104-6145, USA
*Present address: Department of Pediatrics, UCHSC, 4200 E. 9th Avenue, Denver, CO 80262, USA
†Present address: Array BioPharma, 3200 Walnut St., Boulder, CO 80301, USA
‡Present address: EMBL Heidelberg, Meyerhofstrasse 1, Heidelberg D-69117, Germany
§Present address: Dharmacon Research, 1376 Miners Drive, Lafayette, CO 80026, USA
¶Author for correspondence (e-mail: wood@stripe.colorado.edu)

Accepted 30 July 2002

SUMMARY

Co-factor homeodomain proteins such as *Drosophila* Homothorax (Hth) and Extradenticle (Exd) and their respective vertebrate homologs, the Meis/Prep and Pbx proteins, can increase the DNA-binding specificity of Hox protein transcription factors and appear to be required for many of their developmental functions. We show that the *unc-62* gene encodes the *C. elegans* ortholog of Hth, and that maternal-effect *unc-62* mutations can cause severe posterior disorganization during embryogenesis (Nob phenotype), superficially similar to that seen in embryos lacking function of either the two posterior-group Hox genes *nob-1* and *php-3* or the *caudal* homolog *pal-1*. Other zygotically acting *unc-62* alleles cause earlier embryonic arrest or incompletely penetrant larval lethality with variable morphogenetic defects among the survivors, suggesting that *unc-62* functions are required at several stages of development. The differential accumulation of four *unc-62* transcripts is consistent with multiple functions. The *C. elegans exd* homologs *ceh-20* and *ceh-40* interact genetically with *unc-62* and may have overlapping roles in embryogenesis: neither CEH-20 nor CEH-40 appears to be required when the other is present, but loss of both functions causes incompletely penetrant embryonic lethality in the presence of *unc-62(+)* and complete embryonic lethality in the presence of an *unc-62* hypomorphic allele.

Supplemental data available on-line

Key words: Embryonic patterning, Hox proteins, Meis family, PBC family, Transcription factors

INTRODUCTION

Central to the patterning process in all animal embryos are the homeodomain transcription factors known as homeotic selector (Hox) proteins (for a review, see Manak and Scott, 1994). Hox proteins often bind target DNA sites in vitro with little selectivity (Ekker et al., 1994; Hoey and Levine, 1988; Mann, 1995). Their biological specificity appears to depend on interactions with protein co-factors, some of which are members of the TALE (three amino acid loop extension) class of atypical homeodomain proteins. These proteins are further divided into families based on similarities in a more N-terminal domain (Burglin, 1997), which is believed to be important for protein interactions (Abu-Shaar et al., 1999). *Drosophila* Extradenticle (Exd) and its vertebrate homologs the Pbx proteins, which are characterized by bipartite PBC-A and PBC-B interaction domains, comprise the PBC family. *Drosophila* Homothorax (Hth) and its vertebrate homologs the Meis/Prep proteins include the Hth/Meis (HM) interaction domain and are referred to as the Meis family (reviewed by Mann and Affolter, 1998; Mann and Chan, 1996).

In the PBC family, Exd can associate with and increase the binding specificity of the medial-group Hox proteins Ultrabithorax and AbdA, but not the posterior-group protein AbdB (Chan et al., 1994; van Dijk and Murre, 1994). Likewise, the homologous vertebrate Pbx proteins can increase the binding specificity of the first 10 Hox paralog proteins, including the posterior-group Hox9 and Hox10 proteins, but not that of the posterior-group Hox11-Hox13 proteins (Shen et al., 1997b). In the Meis family, the vertebrate Meis/Prep proteins associate with and increase the binding specificity in vitro of Hox9-Hox13 proteins (Shen et al., 1997a).

The PBC- and Meis-family Hox co-factors in turn appear to be co-regulated through subcellular localization (Pai et al., 1998). Exd, which includes both nuclear localization and nuclear export signals in its sequence (Rieckhof et al., 1997), is retained in the cytoplasm after synthesis. Complexing with Hth, however, inactivates the export signal, and the complex becomes localized to the nucleus where it can interact with Hox proteins (Abu-Shaar et al., 1999; Ryoo et al., 1999; Affolter et al., 1999). Analogous studies in vertebrates have

demonstrated similar interactions between the Pbx and Meis/Prep proteins (Berthelsen et al., 1999; Ryoo et al., 1999), suggesting that this may be a well-conserved mechanism for regulating Hox gene function.

C. elegans has six Hox genes, three of which have known patterning roles during larval development (Chisholm, 1991; Clark et al., 1993; Wang et al., 1993). However, relatively little is so far known about earlier Hox gene functions during embryonic development. In contrast to the situation in *Drosophila* and vertebrates, only anterior- and posterior-group Hox paralogs, *ceh-13* (Brunschwig et al., 1999) and *nob-1*/*php-3* (Van Auken et al., 2000), respectively, are essential for embryonic patterning and viability. Neither the medial-group homologs *mab-5* and *lin-39*, nor the posterior-group homolog *egl-5* are required for embryonic survival (Chisholm, 1991; Clark et al., 1993; Wang et al., 1993); even embryos lacking function of all three of these genes develop into larvae that exhibit patterning defects but nevertheless survive to become fertile adults (Wrischnik and Kenyon, 1997).

In screens for *C. elegans* embryonic lethal patterning mutants (Edgar et al., 2001), we found a loss-of-function maternal-effect mutation in the *unc-62* gene that causes severe posterior defects (Nob phenotype) superficially similar to those of *nob-1/php-3* embryos (Van Auken et al., 2000) and embryos lacking zygotic function of the *caudal* homolog *pal-1* (Edgar et al., 2001). We show here that *unc-62* is the *C. elegans* ortholog of *Drosophila hth* (previously known as *ceh-25*) (Burglin, 1997), and that its transcripts include four splice variants predicted to encode proteins with two alternative homeodomains and strong similarity to the Meis family of Hox co-factors. We have molecularly characterized six *unc-62* alleles and have analyzed the resulting phenotypes, which range from the originally reported uncoordinated (Unc) phenotype (Brenner, 1974) through larval defects and lethality to early embryonic arrest. Our results suggest multiple functions for *unc-62* gene products.

We have also shown that both of the two *C. elegans* PBC-family members, *ceh-20* and *ceh-40*, interact genetically with *unc-62*. Although embryos lacking either *ceh-20* or *ceh-40* alone are viable, loss of both functions causes embryonic lethality that is strongly enhanced by a hypomorphic *unc-62* allele, suggesting overlapping roles for these three genes during embryogenesis.

MATERIALS AND METHODS

Strains and alleles

C. elegans strains, all derived from the Bristol N2 wild type, were obtained from the *Caenorhabditis* Genetics Center or from our collection unless otherwise indicated. Stock maintenance, genetic mapping and complementation tests were carried out using standard methods (Sulston and Hodgkin, 1988).

Genes and alleles referred to are as follows, by linkage group (LG).

LGI: *smg-1(r861)*, *glp-4(bn2ts)*;

LGIII: *fem-2(b245ts)*, *ceh-20(ay38)*, *nDf16* (a small deficiency that uncovers *ceh-20*);

LGIV: *fem-1(hc17ts)*, *him-8(e1489)*;

LGV: *dpy-11(e224)*, *unc-46(e177)*, *unc-62(ct344*, *e644*, *e917*, *ku234*, *s472*, *t2012*), *unc-60(m35)*, and the deficiencies *sDf26*, *sDf27*, and *sDf50*;

LGX: *ceh-40* (predicted gene; no reported alleles).

The *eT1 (III;V)* reciprocal translocation was used as a balancer chromosome for *unc-62* alleles. The duplication *svDp1*, derived from *sDp3* by fusion with a *sur-5::GFP* reporter construct (S. Tuck, personal communication), was used to balance *ceh-20* alleles.

The canonical *unc-62(e644)* was originally described by Brenner (Brenner, 1974). Previously undescribed alleles, characterized by failure to complement *e644*, were obtained as follows: *ct344* from our mutant screens (Edgar et al., 2001), *ku234* in a screen for defects in vulval morphogenesis (M. S. and M. Han, unpublished), and *e917*, *s472* (Rosenbluth et al., 1988) and *t2012* as gifts from A. Chisolm, D. Baillie, and R. Schnabel, respectively.

All *unc-62* mutations were outcrossed at least three times; *s472* was outcrossed ten times prior to phenotypic analysis. Homozygous lethal mutations were balanced over *eT1 (III;V)* or over LGV doubly marked with *unc-60* and *dpy-11*. The *s472* deletion mutation was maintained as *unc-62(s472) unc-46(e177)/unc-60(m35) dpy-11(e224)*; presence of the *s472* deletion was verified by PCR.

To determine whether the strong *ceh-20* allele *ay38* (kindly supplied by M. Stern) is likely to be a null mutation, we used direct PCR sequencing to show that it is a C→T transition predicted to cause premature termination of translation (Q102→stop, as also found by E. Chen and M. Stern, personal communication) near the start of the PBC-B domain. Genetic tests in an *unc-62(e644)* background showed that homozygous *ceh-20(ay38)* results in higher lethality than either *ceh-20(RNAi)* or the hemizygous mutant *ceh-20(ay38)/nDf16*. Moreover, heterozygous *ay38/+* caused a dominant enhancement of lethality, and *ay38/ay38/+* caused a more severe dominant enhancement. These results indicate that *ay38* exhibits antimorphic character in this background and, therefore, is not a null allele (data available on request).

Viability assays

Embryonic and larval lethality were scored by allowing hermaphrodites to lay eggs for 24 hours (20°C) and then transferring the parents to a new plate daily for the next 3-4 days. Twenty-four hours after the hermaphrodite was removed from a plate, all progeny were scored for viability by counting unhatched embryos and living larvae. To assess lethality at later larval stages, surviving animals were followed until they died or became fertile adults.

Microscopy and lineage analysis

Phenotypic analyses and immunofluorescence microscopy were carried out as described (Edgar et al., 2001) using a Leitz microscope equipped with Nomarski optics and UV epi-illumination. Antibodies to LIN-26 and MHC-A were kindly provided by M. Labouesse and R. Waterston, respectively; an integrated *jam-1::GFP* reporter construct was obtained from M. Han; the *ceh-20::GFP* reporter construct pHK110, including 2.2 kb of *ceh-20* promoter sequence and encoding full-length CEH-20 fused at the C terminus with GFP, was kindly provided by H. Kagoshima and T. Burglin. Lineage analysis was performed with a multi-focal-plane time-lapse video recording system (Thomas et al., 1996); embryos were typically recorded for 5-6 hours post-fertilization at 22°C.

Identification of unc-62 lesions

Genomic DNA fragments were amplified using suitable PCR primers across a ~27 kb region containing *unc-62*. All *unc-62* lesions were identified and confirmed by direct PCR sequencing. For *s472*, the proximal and distal endpoints are located in the sequences TAAGTTGTCCTTAGTCTTATTAAAA and GCTTTGTGTGTGTG-TGAACAGTTAT, respectively (underlined bases are deleted). For *ct344*, the proximal and distal endpoints are located in the sequences ACTTCAAACGATCAAATAATGATTT and CGGGTTTACAGCC-CTGAATAGGTT, respectively. The *e917* molecular lesion was identified as a probable inversion by inverse PCR sequencing of re-ligated Sau3AI fragments of *e917* genomic DNA; inversion was confirmed by direct PCR sequencing across the break points. One

break point was located in the *unc-62* region of LGVL (cosmid T08H10), 8.25 kb upstream of the exon 1a start codon (see Fig. 6); the other was found on the right arm of V (included in YAC Y40H4A). For additional characterization of this rearrangement, see supplemental data at http://dev.biologists.org/supplemental/.

RNA interference, RNA blots and quantitative PCR

RNAi was performed essentially as described (Montgomery et al., 1998; Tabara et al., 1998). cDNA templates were either obtained from Y. Kohara (*unc-62* and *ceh-20*) or generated by RT-PCR from *C. elegans* embryonic total RNA, and were transcribed using standard methods prior to annealing to produce double-stranded (ds) RNA. dsRNA was used either for injection (Montgomery et al., 1998) or soaking (http://nematode.lab.nig.ac.jp/db/rnai_s/RNAiBySoaking.htm) (spermidine and gelatin were omitted from the soaking mix) at concentrations of 0.2-1.0 mg/ml. Progeny embryos scored for viability and subsequent larval defects were collected during a 24-96 hour period after injection or a 48-96 hour period after soaking.

For RNA blots total RNAs from the populations described below were isolated, run on formaldehyde gels and blotted onto Hybond-N membranes (Amersham) as described previously (Streit et al., 1999).

For quantitative PCR RNA samples were reverse transcribed with an *unc-62* gene-specific primer using SuperScript II™ (Invitrogen) under conditions described by the manufacturer. PCR assays with primer pairs recognizing common sequences near the 3′ and 5′ ends of the mRNAs showed that full-length cDNAs had been generated. Each cDNA sample was then amplified in triplicate with four transcript-specific primer pairs as well as a reference primer pair common to all four transcripts. Amplification reactions were carried out simultaneously in an ABI Prism 7700 Sequence Detection System, using SYBR® Green PCR Master Mix (Applied Biosystems) to allow the course of each reaction to be followed. Using the mean values from each set of three reactions, ratios of each individual transcript to total *unc-62* mRNA were determined. The relative ratios were calculated by the $2^{\Delta\Delta}C_T$ method (Livak and Schmittgen, 2001), using the common reference primer pair as the internal control and the EE sample as the calibrator for each primer pair.

GenBank Accession Numbers

Accession numbers for the four *unc-62* transcripts 1a-7a, 1a-7b, 1b-7a and 1b-7b are AF427474, AF427475, AF427476 and AF427477, respectively.

RESULTS

unc-62 is the *C. elegans* Meis-family homeobox gene

The *unc-62(e644)* mutation was mapped to a small interval on the left arm of LGV (Fig. 1A). This region includes the homeobox gene *ceh-25*, which encodes the only *C. elegans* homolog of *Drosophila* Hth, a Meis-family member of the TALE class of homeodomain proteins (Burglin, 1997). We established that *ceh-25* was *unc-62* by identifying molecular lesions associated with this gene for six *unc-62* alleles, as described below. We will refer to this gene henceforth as *unc-62*.

Sequencing of five *unc-62* cDNA clones from the *C. elegans* EST collection, as well as RT-PCR and 5′-RACE products confirmed the general gene structure predicted by Burglin (Burglin, 1997). However, our analysis revealed a second start exon 5′ to that predicted originally, and also showed that the 5′ end of exon 7a is 249 bp downstream of the originally predicted position (Fig. 1B). The 12 exons of *unc-62* are distributed over about 15 kb of DNA. The sequencing revealed four alternative transcripts that differ in choice of the first exon (1a or 1b) and the seventh exon (7a or 7b). 5′-RACE analysis showed no evidence for any further upstream exons, but demonstrated that exon 1a is trans-spliced to the splice leader SL1, while exon 1b is not. Exons 7a and 7b encode alternative polypeptide sequences that include the most N-terminal region of the homeodomain. Of the two, the 7a-encoded sequence is more similar to the *Drosophila* Hth and murine Meis homeodomains. Three of the five cDNA clones sequenced were full length; two of these contained exon 1a and one contained exon 1b. However, all five cDNAs contained exon 7b; transcripts containing exon 7a were detected only by RT-PCR. No transcripts were detected that contained both 7a and 7b. The four alternative transcripts will be referred to subsequently as 1a-7a, 1a-7b, 1b-7a and 1b-7b, respectively (see Materials and Methods for GenBank Accession Numbers).

Differential accumulation of *unc-62* transcripts

RNA blot analysis of stage-specific total RNA with transcript-specific probes showed different accumulation patterns for the four *unc-62* mRNAs (Fig. 2A). The 1a-containing mRNAs were more abundant than the 1b-containing mRNAs, but their temporal patterns of accumulation appeared similar. Both were present in adult germline, pregastrulation embryos, later embryos and adult soma. The 7a signals were too weak to assess relative abundances at different stages. The 7b-containing mRNAs appeared much more abundant than the 7a RNAs in both embryos and adults

Non-uniformity of sample loading made quantitation from RNA blots difficult (Fig. 2A). Further evidence for differential accumulation was obtained using quantitative real-time PCR analysis (QPCR) with appropriate transcript-specific primers (Giulietti et al., 2001; Livak and Schmittgen, 2001). These experiments allowed us to compare the ratio of each transcript to total *unc-62* mRNA at later stages relative to this ratio in early embryos. The results, summarized in Fig. 2B, are consistent with the RNA blot results, but also show that the levels of the rare 7a transcripts increase over 100-fold from early embryos to adulthood. In addition, the QPCR results show that the levels of 7b mRNAs (unclear from the RNA blot because of non-uniform loading) are approximately the same in adult soma and complete adults, indicating that both 7b and 7a mRNAs are present in adult soma. The lower relative levels of 7a mRNAs in complete adults compared with adult soma raises the possibility that 7a mRNAs are not present in the hermaphrodite germline.

Functional tests for differential transcript requirements during development were attempted using RNAi with four transcript-specific dsRNAs, prior to the publication of evidence for spreading of RNAi that makes such experiments unlikely to be informative (Lipardi et al., 2001). The dsRNAs used had to be small in order to be transcript specific, and did not cause significant phenotypic defects (data not shown).

Molecular lesions in *unc-62* mutants

The six mutants analyzed phenotypically (see following section) included a severe zygotic embryonic lethal (*s472*), two mutants with weaker zygotic effects (*e644, ku234*) and three primarily maternal-effect lethal mutants of different severities. Sequencing of *unc-62* from mutant strains revealed molecular

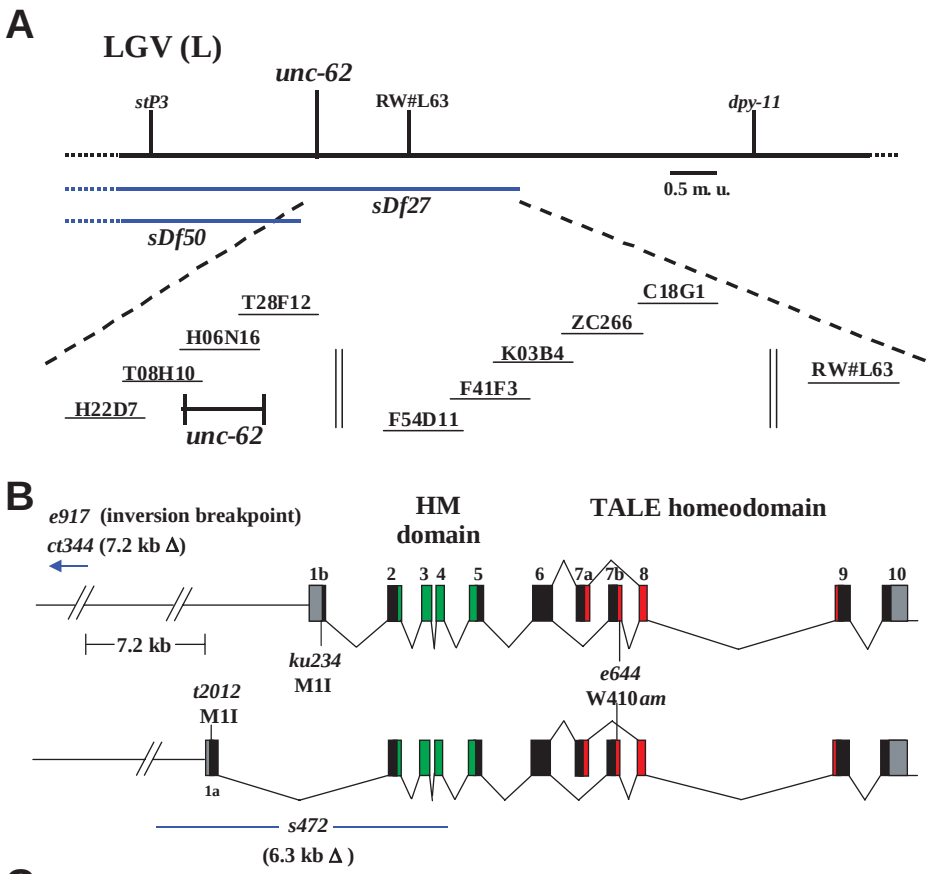

Fig. 1. *unc-62* molecular cloning, transcript structure and sequence comparisons. (A) Genetic and physical maps of the *unc-62* region on LGV. Genetic mapping placed *unc-62* on the left arm of LGV, between two strain-specific polymorphisms *stP3* and *RW#L63* and in the region uncovered by deficiency *sDf27* but not *sDf50*. Cosmids mapped to this region by the *C. elegans* genome consortium are shown below. *unc-62* putative regulatory sequences and coding sequence reside on cosmids T08H10 and T28F12, respectively; both the regulatory and coding sequences are included in the fosmid clone H06N16. (B) Structure of *unc-62* transcripts and locations of mutant lesions. *unc-62* produces four alternatively spliced transcripts that differ in the choice of the first exon (1a or 1b) and the seventh exon, which is the first exon of the homeobox region (7a or 7b). The HM domain is encoded by exons 2, 3, 4 and 5, while the TALE homeodomain is encoded by exons 7a or 7b, 8 and 9. Locations of the point mutations *t2012* and *e644*, the deletions *s472* and *ct344*, and the left inversion breakpoint of *e917* are indicated (see Fig. 6 for a more precise map of the rearrangements). (C,D) Sequence similarities of the conserved UNC-62, Homothorax, and murine Meis1 HM and homeodomains, respectively. Dashes indicate identical residues.

lesions corresponding to all six of these alleles. Three of the mutations affect coding sequence, and two affect upstream putative regulatory sequences (Fig. 1B).

The severe zygotic allele *s472* is a 6.3 kb deletion that removes 1.6 kb of upstream sequence, both alternative first exons 1a and 1b, and exons 2, 3 and 4, which encode most of the HM domain. This allele seems likely to be a molecular null. The weaker zygotic allele *e644* is a single base transition that changes the Trp410 (TGG) codon to a stop (TAG) codon in the alternatively spliced exon 7b, corresponding to the 19th residue of the homeodomain (Fig. 1D). The resulting transcript should be degraded by the *smg* system for nonsense-mediated decay (Pulak and Anderson, 1993). A test for effects of inactivating the *smg* system on phenotypes resulting from the *e644* mutation showed a substantial increase in viability, from 29% (n=968) in the original *smg(+)* strain to 69% (n=932) in a *smg-1* mutant background. Therefore, *e644* is acting as a hypomorphic rather than an antimorphic allele. The weakest zygotic allele *ku234* is a single base transition that changes the predicted initial Met (ATG) codon in exon 1b to an Ile (ATA) codon. The next predicted Met codon does not occur until the 39th codon of the 1b transcript, 16 codons before the start of the HM-domain coding region in exon 2 (Fig. 1C).

The most severe of the maternal-effect lethal mutations, *t2012*, is a single base transition that changes the first possible translational start in exon 1a from a Met (ATG) to an Ile (ATA) codon. The next predicted Met codon is in exon 2 as indicated above; this is codon 73 of the exon 1a transcript. The less severe maternal-effect lethal mutation *ct344* is a 7.2 kb deletion, beginning 7.2 kb upstream of exon 1a. The deletion removes ~3.6 kb of potential *unc-62* regulatory sequence, as well as a putative upstream gene (T08H10.1), which is predicted to encode the enzyme aldose reductase. In RNAi

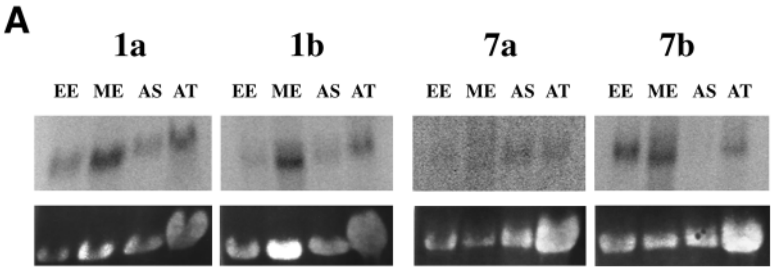

B

1a				1b				7a				7b			
EE	ME	AS	AT	EE	ME	AS	AT	EE	ME	AS	AT	EE	ME	AS	AT
1	0.6	0.6	0.1	1	5	2	0.6	1	8	500	100	1	1	0.4	0.3
0.78-1.3	0.37-0.83	0.34-0.95	0.04-0.38	0.64-1.6	3.1-7.3	1.1-4.0	0.32-1.3	0.58-1.7	7.7-9.1	310-800	56-200	0.67-1.5	1.0-1.2	0.29-0.47	0.14-0.65

Fig. 2. (A) Blots of RNA from early (pregastrulation) embryos (EE), mixed-stage embryos (ME), adult soma (AS) and adult total (AT) hybridized to four transcript-specific probes. EE: >90% pregastrulation embryos (Schauer and Wood, 1990). ME: mixed-stage embryos isolated by hypochlorite treatment of *him-8(e1489)* hermaphrodites. AS: *glp-4(bn2ts)* young adult hermaphrodites that had been shifted to non-permissive temperature (25°C) at hatching; these animals lack almost all germline cells (Beanan and Strome, 1992). AT: *fem-2(b245ts)* young adult hermaphrodites that had been shifted to non-permissive temperature (25°C) for 36 hours after hatching (the temperature-sensitive period), then returned to permissive temperature; these animals produce no sperm and therefore contain oocytes but no fertilized embryos (Kimble et al., 1984). Photographs of 18S rRNA UV absorption bands on the blots before probing are shown as loading controls (lower panels). The fourth (AT) lane of each gel is clearly overloaded relative to the other three. In preliminary experiments using equal specific activities for the 1a and 1b probes, the 1b bands were fainter than the 1a bands. In the experiment shown, a 1b probe at about twice the specific activity of the 1a probe was used in order to better compare band intensities among the four RNA preparations. (B) Results of real-time quantitative PCR experiments to compare the relative ratios of each transcript with total *unc-62* mRNAs in the same RNA populations as analyzed in A. Figures in the table represent the ratio obtained for each primer pair relative to the ratio obtained for the EE sample, which was arbitrarily assigned a value of 1.0. The ranges shown for each ratio were calculated from the results for each triplicate set according to User Bulletin #2: ABI Prism 7700 Sequence Detection System (2001). This experiment was carried out three times with similar results; ratios and ranges shown in the figure are from one experiment.

experiments, injection of N2 hermaphrodites with dsRNA made using a 0.9 kb cDNA for this gene caused increases of only 5% embryonic and 4% subsequent larval lethality over controls (*n*=1193 progeny), suggesting that loss of T08H10.1 function in *ct344* does not contribute significantly to the resulting phenotype. The third maternal-effect lethal mutation, *e917*, is a complex chromosomal rearrangement (see Materials and Methods; see supplemental data at http://dev.biologists.org/supplemental/). One inversion breakpoint occurs 8.25 kb upstream of exon 1a, within the region deleted by the *ct344* mutation, while the other is on the right arm of LGV.

unc-62 mutations result in a variety of phenotypes

The deletion allele *s472* causes 100% zygotic lethality among the homozygous progeny of heterozygous hermaphrodites. Of these, 84% die as unhatched embryos, some of which fail to enclose completely and rupture at elongation [Table 1; Fig. 3A; supplemental Fig. S2 (at http://dev.biologists.org/supplemental/)]. The remaining 16% survive to hatching but display a variety of morphological defects consistent with failures of hypodermal and muscle patterning and differentiation. Lineage analysis (*n*=3) showed misaligned cleavages and mispositioning of the C (dorsal) and V (lateral seam cell) precursors as early as the 100-cell stage, resulting in V cells in dorsal positions and C cells more lateral and posterior than in wild-type embryos, as described below for the two strong maternal-effect alleles (Fig. 4B). C muscle precursors were also mispositioned (*n*=1). Ventral cleft closure, the last stage of gastrulation (at ~300 cells), was incomplete at the posterior in two out of three embryos lineaged. In three out of three, subsequent hypodermal enclosure was delayed and a few cells were extruded [supplemental Fig. S2 at (http://dev.biologists.org/supplemental/)]. These embryos failed to elongate. Mutant *s472* embryos expressing a JAM-1::GFP reporter, which localizes to the tight junctions between hypodermal cells, showed variable hypodermal cell defects: seam cells could be reduced in number, not touching or grouped in patches (Fig. 4G,H). In contrast to *nob-1* embryos (Van Auken et al., 2000), the gut (E) lineage appeared normal (*n*=1).

The canonical allele *e644*, in addition to the originally described Unc phenotype (Brenner, 1974), results in zygotic defects that cause 20% lethality among the homozygous mutant progeny of heterozygous hermaphrodites, primarily during larval stages (Table 1). The *e644* homozygotes that survive to adulthood exhibit a much higher level (67%) of progeny lethality (Table 1), indicating a significant maternal effect. Some of these progeny die as embryos, but about half are inviable larvae with variable phenotypes, some of which probably result from abnormal embryonic development (Fig. 3B). The defective embryos show variable misplacement of seam cells and failure of hypodermal cells to fuse normally into hypodermal syncytia (Fig. 4I,J). Surviving *e644* mutant adults display several phenotypes, including Unc, egg-laying-defective (Egl) and variably abnormal larval morphology (Vab). Previous studies suggested that the Unc movement defects may be a result of aberrant axonal outgrowth of motoneurons (Siddiqui, 1990). The Egl animals appear to have normal vulval structures but fail to lay eggs, even when treated with serotonin (5-HT) (data not shown), which stimulates the vulval muscles to promote egg-laying (Thomas et al., 1990; Trent et al., 1983). This result suggests that the Egl animals are defective in vulval muscles rather than vulval innervation. Causes of the Vab phenotype are unknown.

The third non-maternal allele, *ku234*, was isolated in independent screens for Egl mutations (M. S. and M. H., unpublished). Although 13% of the progeny of homozygous

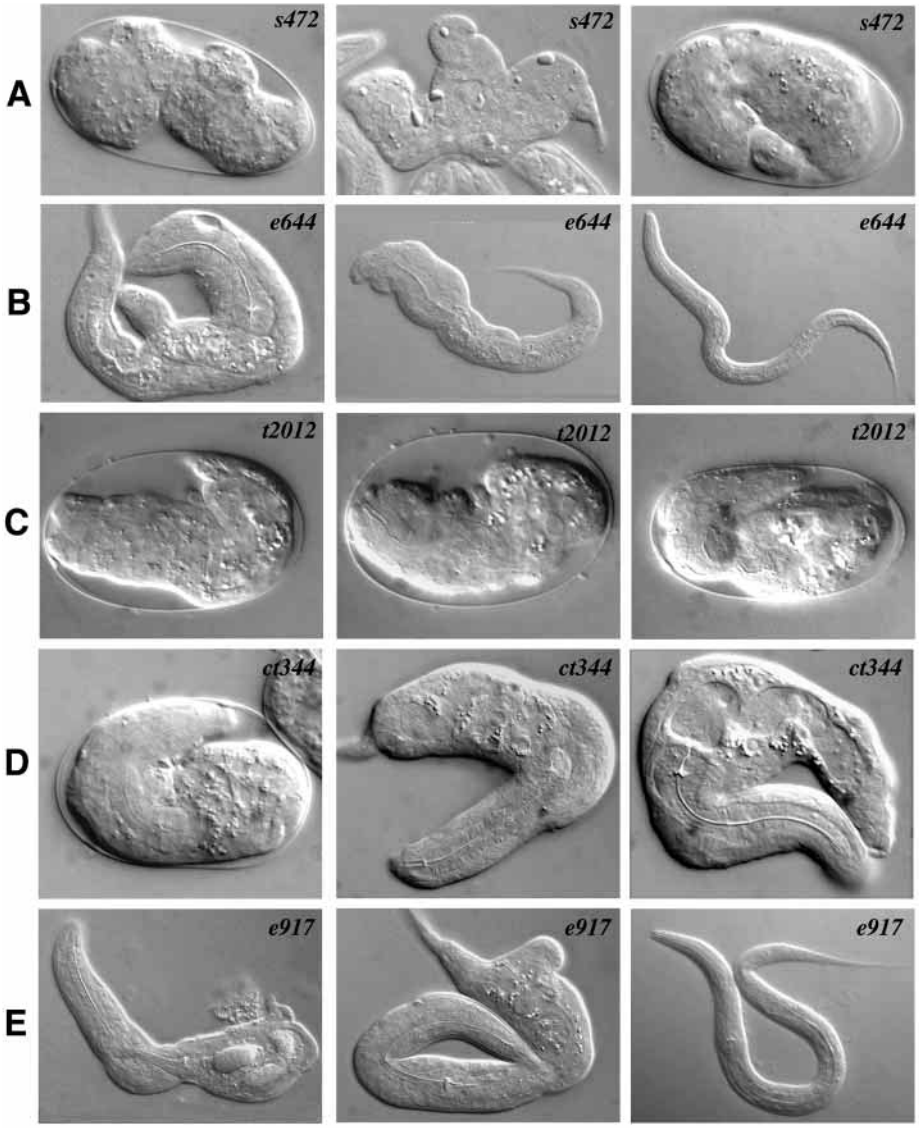

Fig. 3. Late embryonic and larval arrest phenotypes resulting from five *unc-62* alleles. Animals in row A are homozygous mutant progeny of heterozygous *unc-62/+* hermaphrodites; those in rows B-E are progeny of homozygous mutant hermaphrodites. Alleles are indicated in each panel. Each allele results in a range of phenotypes represented by the individuals shown.

ku234 hermaphrodites die as embryos and larvae (Table 1), the survivors exhibit no gross morphological defects during embryonic or larval stages. However, about 50% of the survivors have visible vulval defects (Fig. 5) and 100% are Egl. The vulval phenotypes of *ku234/s472* and the hemizygous *ku234/sDf27* are only marginally more severe than those of *ku234* homozygotes (Fig. 5). The *ku234* mutation was identified as an *unc-62* allele on the basis of its failure to complement *s472* and *e644* (see Materials and Methods and supplemental data at http://dev.biologists.org/supplemental/). However, it does complement the maternal-effect lethal alleles *t2012, ct344* and *e917*.

The three alleles *t2012*, *ct344* and *e917* result primarily in maternal-effect lethality. Although they also exhibit zygotic effects to different degrees, as discussed below, most of the homozygous progeny embryos from hermaphrodites heterozygous for these alleles develop into fertile adults that appear normal (Table 1). These homozygous hermaphrodites produce nearly 100% inviable embryos and defective larvae by self-fertilization. However, when mated to wild-type males, both *t2012* and *ct344* hermaphrodites produce 80-90% viable progeny of genotype *unc-62/+* (Table 2). Similar rescue experiments with *unc-62/+* males indicate that rescue depends on introduction of the + allele (i.e. there is no paternal effect; all surviving progeny are of genotype *unc-62/+*). *e917* hermaphrodites exhibit behavior similar to *t2012* and *ct344* hermaphrodites in both types of experiments (data not shown). Therefore, these three alleles behave as partial (male-rescuable) maternal rather than strict maternal-effect mutations.

For *t2012*, the most severe of the maternal-effect alleles, almost all the self-progeny of homozygous hermaphrodites arrest as unhatched embryos (Table 1). These embryos execute the normal embryonic lineage pattern in terms of timing and numbers of divisions (n=2) and produce differentiated gut, muscle and pharyngeal tissue. However, they exhibit early misplacement of hypodermal precursor cells (Fig. 4C) and generally fail to undergo normal enclosure, elongation and morphogenesis (Fig. 3C). In addition, they fail to produce the normal number of differentiated hypodermal cells in embryos and larvae as identified using antibodies to the hypodermal marker LIN-26 (Labouesse et al., 1996). LIN-26, normally expressed in ~84 cells, was detected (by immunofluorescence using an anti-LIN-26 antibody) in an average of only 64 cells (range 53-75; n=28) among progeny of homozygous *t2012* hermaphrodites. Severe disorganization was seen among these cells in *t2012* mutant embryos expressing the JAM-1::GFP reporter construct (Fig. 4K,L), as well as among body-wall muscle cells visualized with anti-MHC-A (not shown). The *t2012* allele also results in some zygotic lethality (Table 1) with similar gross embryonic phenotypes.

Homozygous *ct344* hermaphrodites produce embryos that generally arrest later than those from *t2012* animals, resulting in roughly equal numbers of unhatched embryos and hatched inviable larvae (Table 1). Embryos usually progress through morphogenesis, but often display a Nob phenotype in which anterior head and pharyngeal structures develop normally, but the posterior is severely malformed (Fig. 3D). As in *t2012* embryos, although the embryonic cell lineage pattern of *ct344*

Table 1. Zygotic and maternal-effect lethality resulting from six *unc-62* alleles*

Row	Maternal genotype	Viability among total progeny: Embryonic arrest (%)†	Viability among total progeny: Larval arrest (%)†	Viability among total progeny: Surviving progeny (%)†	Lethality among *unc-62* homozygous mutant progeny (%)‡
1	+ *unc-62(s472) unc-46(e177)* + / *unc-60(e723)* + + *dpy-11(e224)*	21	4	75	100
2	*unc-62(e644) dpy-11(e224)* / + +	3	9	88	20
3	*unc-62(e644)*§ / *unc-62(e644)*	18	49	33	67
4	*unc-62(t2012) dpy-11(e224)* / + +	5	6	89	8
5	*unc-62(t2012) dpy-11(e224)* / *unc-62(t2012) dpy-11(e224)*	96	4	0	100
6	*unc-62(ct344) dpy-11(e224)* / + +	4	5	91	8
7	*unc-62(ct344) dpy-11(e224)* / *unc-62(ct344) dpy-11(e224)*	57	43	0	100
8	*unc-62(e917)* / +	3	2	95	1-4
9	*unc-62(e917)* / *unc-62(e917)*	57	40	3	97
10	*unc-62(ku234)* / *unc-62(ku234)*	8	5	87	13
11	+ / +	2	2	96	–
12	*unc-46(e177)* / *unc-46(e177)*	2	2	96	–
13	+ *unc-46(e177)* / *unc-60(e273) dpy-11(e224)*	2	ND	ND	–

*Individual embryos from the indicated parental genotypes were picked and scored for hatching at 20°C. Inviable embryos were subtracted from animals that grew to adulthood to determine larval lethality. Between 1000 and 2000 embryos were scored for each genotype.

†The genotype-independent background lethality of 2% embryonic and 2% larval seen in controls (rows 11-13) can be subtracted from lethality and added to viability figures in rows 1-12 to estimate the effects resulting from the genotypes shown. Surviving progeny were defined as those that grew to adulthood.

‡Percent lethality among homozygous *unc-62* mutant progeny of heterozygotes was estimated as follows for the various genotypes. For row 1, no Unc-46 progeny survived; therefore, homozygotes were 100% inviable. For rows 2, 4 and 6 the percentages of Dpy survivors among total progeny were 19%, 22% and 22%, respectively. If Dpys, which are assumed to represent 25% of progeny, die at the control frequency of 4%, then the expected percentage of Dpy survivors among total progeny would be 24%. The discrepancy between this and the observed value represents the missing Dpy animals, and can be divided by 25% to give the percentage of lethality among homozygous mutant progeny. Thus in row 2, for example, the discrepancy is 5% (24% versus 19%), which indicates 5/25 or 20% lethality among homozygotes. For row 8, these calculations could not be made as no marker was present. Thus, 1% is the minimum homozygote lethality if homozygotes were at no disadvantage; 4% is the maximum if only homozygotes failed to survive.

§A similar experiment with *unc-62(e644) dpy-11(e224)* gave similar results (Table 3, row 7).

embryos appears normal (*n*=2), hypodermal precursors are misplaced by the early gastrulation stage (Fig. 4D), and hypodermal cells are under-represented and grossly disorganized in Nob larvae, as if they fail to differentiate properly (Fig. 4M,N). The *ct344* allele also results in some zygotic lethality (Table 1) with similar gross embryonic phenotypes.

Table 2 shows the lethality resulting from heteroallelic genotypes derived from *e644*, *t2012* and *ct344*. Heteroallelic *ct344/t2012* embryos are all inviable, regardless of the parental origins of the two alleles. Interestingly, however, *t2012/e644* embryos are >50% viable if *t2012* is introduced from the male parent, but 0% viable if the maternal parent is homozygous for *t2012*. Such non-reciprocality is not observed for *ct344/e644* embryos; their viability is similar to that of *e644* embryos regardless of the parental origin of *ct344*. These results are consistent with other observations that *ct344* is a weaker allele than *t2012*.

The third maternal-effect allele *e917* is similar to *ct344* in the percentages of embryonic and larval lethality among the self progeny of homozygous hermaphrodites (Table 1). However, the resulting larvae appear to be generally less defective morphologically (Fig. 3E). The ~3% that survive to be fertile adults display a variety of defects including Egl, Unc

Table 2. Lethality resulting from heteroallelic combinations of *unc-62* alleles*

Row	Maternal genotype		Paternal genotype	Embryonic arrest (%)	Larval arrest (%)	Viable (%)	*n*
1	*e644*/*e644*	self	NA†	9	37	54	352
2	*e644*/*e644*	×‡	+ +	1	1	98	1093
3	*e644*/*e644*	×	*ct344 dpy-11*§	12	29	59	298
4	*e644*/*e644*	×	*t2012 dpy-11*§	20	27	53	202
5	*e644* +/*ct344 dpy-11*	self	NA	16	31	53	794
6	*e644* +/*t2012 dpy-011*	self	NA	10	62	28	677
7	*ct344 dpy-101*	self	NA	57	42	<1	1353
8	*ct344 dpy-11*	×	+ +¶	13	1	86	503
9	*ct344 dpy-11*	×	e644§	14	21	64	285
10	*ct344 dpy-11*	×	*t2012 dpy-11*§	41	59	0	105
11	*ct344 dpy-11*/*t2012 dpy-11*	self	NA	90	10	0	336
12	*t2012 dpy-11*	self	NA	96	4	0	534
13	*t2012 dpy-11*	×	+ +¶	10	1	89	1000
14	*t2012 dpy-11*	×	*ct344 dpy-11*§	64	36	0	173
15	*t2012 dpy-11*	x	*e644*§	76	24	0	165
16	+	self	NA	<1	<1	>99	>1000
17	+	×	+ +¶	4	2	94	474

*Experiments in this table were carried out independently by a different investigator from those in Table 1. Discrepancies in comparable results between the two tables are at least partly due to differences in scoring methods and criteria.

†Not applicable.

‡Hermaphrodites of the indicated maternal genotype were mated with males of the indicated paternal genotype.

§Male was heterozygous [*unc-62(paternal)*/+]. The *unc-62* heteroallelic mutant cross progeny could be distinguished as Dpy in crosses between *dpy-11* hermaphrodites and *dpy-11*/+ males, and as Unc progeny in crosses involving *e644* and either *t2012* or *ct344*, because *e644/t2012* and *e644/ct344* animals exhibit the Unc-62 phenotype. Wild-type cross progeny [*unc-62(maternal)*/+] were not included in these counts and all embryonic lethality was attributed to the *unc-62(maternal)/unc-62(paternal)* genotype.

¶Hermaphrodites carried the *fem-1(hc17ts)* mutation and were reared at 25°C to cause self-sterility. Males were of genotype *him-8(e1489)*.

and Vab. This allele causes almost no zygotic lethality (Table 1), but the homozygous progeny of heterozygous hermaphrodites display the Egl phenotype. Because *e917* is a complex rearrangement as described above and could affect other genes besides *unc-62*, the resulting phenotypes were not analyzed in detail.

The *C. elegans* PBC-family genes *ceh-20* and *ceh-40* may function redundantly during embryogenesis

To test whether the strong interactions observed between MEIS- and PBC-family proteins in both *Drosophila* and vertebrates (see Introduction) might also occur in *C. elegans*, we first analyzed loss of function phenotypes for the *C. elegans* PBC-class gene *ceh-20*. Preliminary characterization of the strong *ceh-20* allele *ay38* indicated that it is probably antimorphic (see Materials and Methods) and thus inappropriate for interaction studies. A previous description by Liu and Fire (Liu and Fire, 2000) of the *ceh-20(RNAi)* phenotype, which they concluded to be null, reported failure of post-embryonic development in the M lineage but little or no embryonic lethality. We obtained similar results (Table 3, rows 4 and 5), suggesting that *ceh-20* is not essential during embryogenesis.

However, there is a second PBC-family homolog in *C. elegans*, the predicted gene *ceh-40*. The predicted protein products of the two genes are 41% identical overall and 74% identical in the homeodomain (Burglin, 1997), suggesting that *ceh-20* and *ceh-40* might function redundantly. No *ceh-40* mutations have been described, and no *ceh-40* cDNAs were found in current databases. However, microarray experiments have shown that *ceh-40* transcripts, absent maternally, appear in embryos at low levels around the onset of gastrulation (L. R. Baugh and C. P. Hunter, personal communication). A *ceh-40* cDNA was obtained using RT-PCR with embryonic mRNA, allowing us to confirm the splice sites of the exons predicted from genomic sequence. When *ceh-40(RNAi)* was carried out

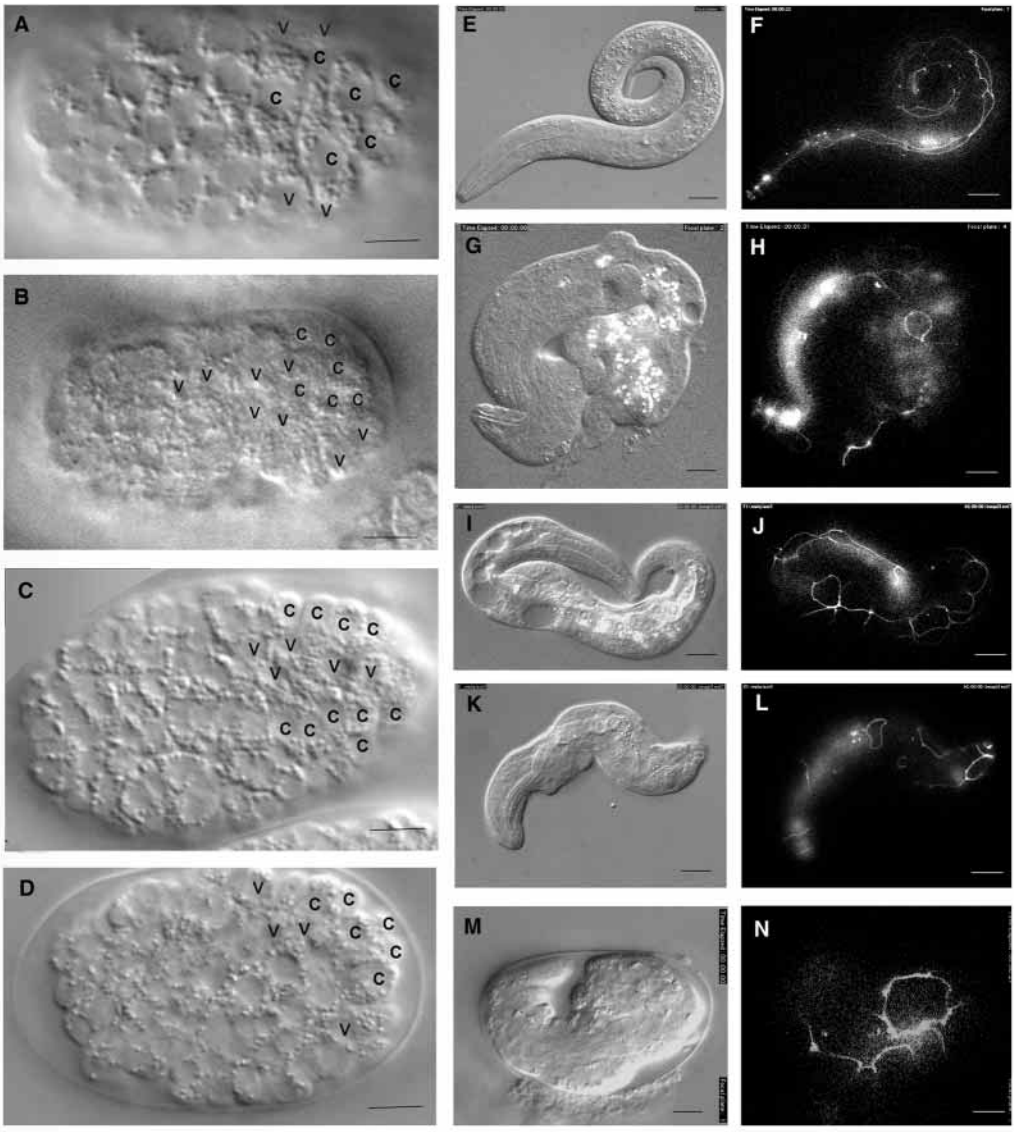

Fig. 4. Aberrant organization of early embryonic dorsal hypodermal and seam cell precursors and the resulting differentiated cells in *unc-62* mutant embryos. Scale bars represent ~10 μm. (A-D) Nomarski images of embryos (dorsal or ventral view, dorsal focal plane, anterior leftwards) that were lineaged to identify cells and photographed about 4 hours post-fertilization (22-25°C). Precursors of hypodermal cells derived from the C lineage and seam cells derived from V lineages are positioned as indicated. (A) Wild-type embryo. Note that dorsal C-derived hypodermal precursors are flanked by V-lineage cells. (Although this embryo is shown approximately one division earlier than the other embryos, the relative position of dorsal midline C hypodermal cells and lateral V precursors is already established at this time, and does not change.) (B) *s472* mutant embryo. Some of the C hypodermal precursors lie abnormally ventral to this focal plane, and are not visible. (C) *t2012* mutant embryo. (D) *ct344* mutant embryo. Embryos in B-D are about one division later than the embryo in A. Relative positions of the C- and V-derived hypodermal cells are aberrant in the three mutants. (E-N) Nomarski and fluorescent images (lateral views, surface focal plane, anterior leftwards) of embryos and larvae expressing JAM-1::GFP, a marker for hypodermal cell junctions. (E,F) Wild-type newly hatched L1, showing the normal expression of JAM-1 at the borders of the row of seam cells. The dorsal and ventral hypodermal cells have fused into syncytia, showing no cell boundaries. (G,H) *s472* newly hatched L1. There are few outlined cells, which do not show a contiguous seam cell pattern. (I,J) *e644* L1, with a more normal pattern but some dorsal hypodermal cells that have not fused. (K,L) *t2012* newly hatched L1, with disconnected seam cells. (M,N) *ct344* late embryo, with few, abnormally large seam cells.

in N2 animals using dsRNA made from this template, no significant embryonic or early larval lethality was observed (Table 3, row 3). Consistent with redundant function, the combination of *ceh-40(RNAi)* with *ceh-20(RNAi)* caused 21% embryonic lethality (Table 3, row 6), a significant increase over either RNAi alone. However, the phenotypes of the dying embryos were not obviously similar to those resulting from the *unc-62(s472)* null allele. [While this paper was in revision, a similar identification of *ceh-40* was reported by Takacs-Vellai et al. (Takacs-Vellai et al., 2002), who also demonstrated embryonic expression of a *ceh-40::GFP* construct.]

Losses of *ceh-20* and *ceh-40* functions interact strongly with the *unc-62(e644)* mutation to give an *unc-62(null)* phenotype

To test for genetic interactions between the PBC-family genes and *unc-62*, we used the semi-viable *unc-62(e644)* allele (Table 1). Because the variety of abnormal phenotypes observed among *unc-62(e644)* homozygous larvae (Fig. 3) made it impractical to reliably detect enhancement of larval defects, we scored only enhancement of lethality as a measure of *ceh-20(RNAi)* and *ceh-40(RNAi)* interaction. The *unc-62(e644); ceh-40(RNAi)* combination resulted in a slight enhancement of embryonic lethality and overall lethality compared to *unc-62(e644)* alone (Table 3, rows 7 and 8). The *ceh-20(RNAi); unc-62(e644)* combination caused an enhancement of embryonic lethality and a larger increase in overall lethality (Table 3, rows 7 and 9). Most strikingly, the triple combination *ceh-20(RNAi); unc-62(e644); ceh-40(RNAi)* caused high embryonic and overall lethality, similar to that seen with *unc-62(RNAi)* (Table 3, rows 10 and 11). Moreover, the phenotypes of the dying, hatched larvae resembled those resulting from the

Table 3. Interactions between *unc-62*, *ceh-20* and *ceh-40*

Row	Genotype*	Embryonic lethality (%)	Larval lethality (%)†	Viable (%)	*n*
1	N2 control (H_2O, *I*)	2	0	98	1397
2	N2 control (H_2O, *S*)	1	0	99	134
3	*ceh-40(RNAi, S)*	4	0	96	86
4	*ceh-20(RNAi, I)*	2	32	66	927
5	*ceh-20(RNAi, S)*	4	37	59	249
6	*ceh-20(RNAi, S); ceh-40(RNAi, S)*	21	3	76	231
7	*unc-62(e644); dpy-11(e224)*	14	47	39	378
8	*unc-62(e644); ceh-40(RNAi, S)*	20	55	25	201
9	*ceh-20(RNAi, I); unc-62(e644)*	26	70	4	544
10	*ceh-20(RNAi, S); unc-62(e644); ceh-40(RNAi, S)*‡	68	28§	4	1203
11	*unc-62(RNAi, I)*¶	72	21	7	1036

*All RNA injections were into N2 where no other genotype is indicated. *RNAi, I* and *RNAi, S* refer to RNAi by injection and soaking, respectively (see Materials and Methods).

†Includes all inviable larvae, ranging from arrest at hatching to lethality at later stages.

‡Of the 16 injected animals that laid eggs, one produced progeny that were apparently unaffected by injection and were undistinguishable from *unc-62(e644)* progeny; the progeny of this animal were excluded from these results.

§All larvae arrested at hatching and were severely deformed, similarly to *unc-62(s472)* progeny.

¶Carried out with dsRNA corresponding to 1a-7b mRNA.

null allele *unc-62(s472)* (Table 1, Fig. 3) and *unc-62(RNAi)* (Table 3). Other experiments showed that overexpression of *ceh-20* enhanced the lethality and other phenotypes resulting from *s472/+*, *e644*, and *ct344* [see legend to supplemental Fig. S4 (http://dev.biologists.org/supplemental/)].

Additional evidence for interaction was obtained in experiments to test whether nuclear localization of a CEH-20::GFP fusion protein would be affected by *unc-62* defects, as predicted from studies cited in the Introduction showing that *Drosophila* Hth and vertebrate Meis functions are required for nuclear localization of Exd and Pbx proteins, respectively. In wild-type embryos, CEH-20::GFP was found to be expressed in many cells, all of which exhibited nuclear localization. In *unc-62(ct344)*, *unc-62(e644)* and *unc-62(RNAi)* embryos, expression was still widespread, but nuclear localization, like the other mutant phenotypes, was variable, observed in none to about half of the expressing cells [see supplemental Fig. S4 (http://dev.biologists.org/supplemental/)].

DISCUSSION

Maternal and zygotic functions of *unc-62* play roles in embryogenesis

We have established that the locus defined genetically as *unc-62* is the sole *C. elegans* Meis-class homeobox gene, previously designated *ceh-25* (Burglin, 1997). The range of embryonic and larval phenotypes resulting from *unc-62* mutations indicates that *unc-62* serves multiple functions in *C. elegans* development, as does its *Drosophila* homolog *hth* (Kurant et al., 2001). We have confirmed, with one correction, the presence of four predicted alternatively spliced transcripts, and have shown that all are present in both embryos and adults. The molecular analysis suggests that *s472* is null and prevents synthesis of any functional *unc-62* transcripts, and that *t2012, ku234 and e644* prevent or reduce the translation of functional proteins from 1a-, 1b- and 7b-containing transcripts, respectively (see Fig. 1).

Assuming these suggestions are valid, we can make several predictions about the time of synthesis and function of the *unc-62* mRNAs and their translation products. 1a transcripts must be required in the early embryo because the self-progeny of *t2012/t2012* hermaphrodites (lacking 1a) are all inviable. Apparently either maternal or zygotic provision of the 1a-containing transcripts is equally effective in promoting survival, because either the self-progeny *t2012/t2012* embryos from *t2012/+* hermaphrodites or the *t2012/+* cross-progeny embryos from *t2012/t2012* hermaphrodites mated to wild-type males are ~90% viable. 1a-containing transcripts are usually sufficient for survival because 87% of the self progeny of *ku234/ku234* hermaphrodites (lacking 1b) are viable. However, we observe a strong dependence of viability on dose of 1a transcripts. 1a transcripts can be reduced by 75% (*t2012* homozygous progeny of a *t2012/+* heterozygote) and animals are still 90% viable, but a further 25% reduction (*t2012* homozygous progeny of a *t2012* homozygote) results in 100% lethality.

We can infer less about time of synthesis or function of 1b-containing transcripts, which are less abundant than 1a transcripts. As mentioned above, 1b transcripts may be nonessential for viability, as the *ku234* allele causes only 13% lethality. However, their presence can affect viability when levels of 1a transcripts are reduced, based on the difference in viability between *t2012* embryos from *t2012/+* hermaphrodites and *s472* embryos from *s472/+* hermaphrodites. Both these embryos should have only 25% the wild-type level of 1a transcripts, yet the former, which can produce normal levels of 1b transcripts, are 90% viable, while the latter, which can produce no 1b transcripts, are <1% viable. There may be additional differences in transcript levels if the *ku234* and *t2012* missense alleles produce some functional transcripts that the *s472* deletion cannot.

The fact that dose effects may contribute to the phenotypes observed does not eliminate the likelihood of transcript-specific functions. This is demonstrated by the 100% penetrance of the Egl phenotype caused by the weak *ku234* allele when compared with the sporadic appearance of this phenotype resulting from the stronger *e644* allele.

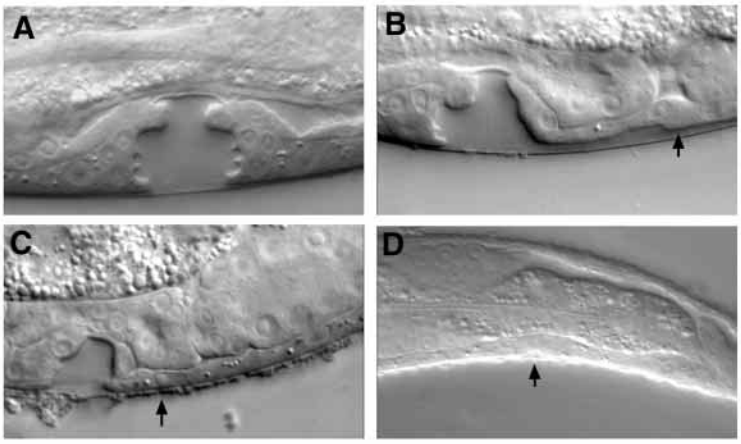

Fig. 5. Examples of aberrant vulval development in *ku234* mutant L4 hermaphrodites. (A) Wild type. (B) *ku234*: descendants of P7.p (arrow) have not joined in the main invagination. About 50% of *ku234* exhibit this phenotype (non-Vul-abnormal), while the rest have apparently normal vulvae. (C) *ku234/s472*: descendents of P7.p (arrow) appear non-vulval. About a third of the non-Dpy segregants from *ku234 dpy-11/unc-62(s472) unc-46* exhibited this semi-vulvaless phenotype, which is only slightly more severe that the non-Vul-abnormal phenotype in B. The remaining non-Dpy animals were either non-Vul-abnormal or normal. (D) *ku234/sDf27*: posterior Pn.p cells appear to be generating vulval-like descendants near the tail (arrow). This phenotype was seen only occasionally. As in C, about a third of the non-Dpy segregants of *ku234 dpy-11/sDf27 unc-46* exhibited the semi-vulvaless phenotype, while the rest were non-Vul-abnormal or normal.

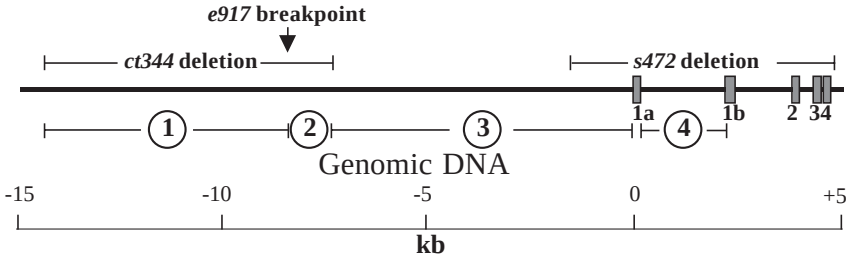

Fig. 6. Physical map of deletion and inversion breakpoints in the vicinity of the *unc-62* promoter, showing numbered regions predicted to include possible regulatory elements (see Discussion). Exon sizes are not to scale.

With regard to the alternative homeodomains encoded by 7a- and 7b-containing transcripts, survival of up to 33% of the self-progeny of *e644/e644* hermaphrodites (deficient in translation products of 7b-containing mRNAs) suggests that the rarer 7a products may compensate for the lack of 7b products. We cannot be confident that 7a products are present in the early embryo, because our quantitative PCR data suggested that 7a-containing transcripts might not be produced maternally (Fig. 2). Alternatively, other proteins with related functions might compensate for 7b products (see discussion of *ceh-20* and *ceh-40* below). Interestingly, molecular analysis of *unc-62* mRNAs in the related nematode *C. briggsae* (estimated time of divergence 15-30 Mya; see supplemental Fig. S3) showed that the splice acceptor sequence for exon 7a appears to be missing, and only transcripts corresponding to 7b could be detected (B. R. and W. B. W., unpublished). This finding supports the suggestion that the 7a and 7b derived proteins in *C. elegans* may have overlapping functions.

The maternal-effect *unc-62* alleles define putative upstream regulatory elements

The *t2012*, *ct344*, and *e917* mutations appear to comprise an allelic series of decreasing severity. All result in maternal-effect lethality that can be rescued by zygotic expression of a wild-type copy introduced from a mating male. The *ct344* allele is less severe than *t2012*, based on generally later arrest of mutant embryos and the finding that progeny of *ct344* hermaphrodites can be rescued by mating to *e644* males, while progeny of *t2012* hermaphrodites can be rescued only by mating to wild-type males. The *e917* allele is even less severe, as indicated by the lack of any zygotic lethality and the observation that 3% of the self progeny from homozygous hermaphrodites survive to reproduce.

Based on the similarity of the phenotypes resulting from these three alleles, they seem likely to affect common functions. Because *t2012* affects translation of 1a-containing mRNAs, while *ct344* and *e917* affect a region ~7 kb upstream of the *unc-62*-coding sequence (Fig. 6), we postulate that *ct344* and *e917* disrupt or remove upstream regulatory elements required for the production of 1a-containing transcripts. Because the *e917* inversion results in a very similar maternal-effect phenotype to *ct344*, at least one such enhancer element may lie between the *e917* breakpoint and the promoter-distal end of the region deleted by *ct344* (Fig. 6, region 1). The zygotic lethality caused by *ct344*, which is not seen with *e917*, suggests that an additional element may lie in the ~1 kb region between the *e917* inversion breakpoint and the proximal end of the *ct344* deletion (Fig. 6, region 2). Additional enhancers may also be present in regions 3 and 4.

The Meis family gene *unc-62* and the PBC-family genes *ceh-20* and *ceh-40* interact genetically

In *Drosophila*, similar phenotypes result from loss of function mutations in the Meis-family homolog *hth* and the PBC-family homolog *exd*, consistent with other evidence for strong interactions between Meis- and PBC-family proteins (see Introduction). Although inactivation of the only previously studied *C. elegans exd* homolog, *ceh-20*, causes only larval and adult defects and no embryonic lethality (Liu and Fire, 2000) (our results above), we have shown that this result may be at least partially due to overlapping functions of two *C. elegans* PBC-family genes, *ceh-20* and *ceh-40*. These two genes interact genetically: *ceh-40(RNAi)* causes no significant embryonic lethality, while *ceh-20(RNAi); ceh-40(RNAi)* causes a substantial decrease in larval lethality with a corresponding increase in embryonic lethality

compared with *ceh-20(RNAi)* alone. In addition, whereas *unc-62(RNAi)* embryos arrest with the Nob phenotype, *ceh-20(RNAi); ceh-40(RNAi)* embryos arrest earlier, prior to morphogenesis. Recent phylogenetic comparisons with similar genes in other nematodes support the view that *ceh-40* may be a *C. elegans exd* ortholog (A. Aboobaker, personal communication). The RNAi results suggest that *ceh-20* and *ceh-40* functions may overlap, with *ceh-40* normally functioning earlier than *ceh-20*. The incomplete penetrance of the *ceh-20(RNAi); ceh-40(RNAi)* lethality compared with the complete penetrance of *unc-62(s472)* or *unc-62(RNAi)* lethality could indicate either that silencing by RNAi was incomplete, or that the functions of *ceh-20* and *ceh-40* are not essential for *unc-62* function as *exd* is essential for *hth* function in *Drosophila*.

In the background of the hypomorphic *unc-62(e644)* allele, which is predicted to reduce or eliminate production of a functional protein from 7b-containing transcripts, *ceh-20* and *ceh-40* show a pattern of interaction with each other similar to that described above. Individually, their RNAi phenotypes are roughly additive to the *unc-62(e644)* phenotype. However, the triple combination of *ceh-20(RNAi); unc-62(e644); ceh-40(RNAi)* results in complete embryonic inviability, with terminal phenotypes similar to those caused by the null allele *unc-62(s472)*. One interpretation of these results is that when levels of the putatively interacting UNC-62 and CEH-20/CEH-40 proteins both fall below some threshold level, the result is a strong Unc-62 phenotype. A more intriguing possibility is that there is some overlap in the functions of CEH-20/CEH-40 and the UNC-62 proteins encoded by 7b-containing transcripts. Perhaps, for example, the latter could act directly as a Hox transcription cofactor.

Possible functions of UNC-62 proteins in embryogenesis

Is UNC-62 a co-factor for the posterior-group homeodomain transcription factors NOB-1 and PHP-3 in embryonic development, as might be expected from findings in other organisms? Table 4 summarizes characteristics of Nob phenotypes resulting from strong *lf* mutations in *unc-62* and *nob-1/php-3* as well as, for comparison, the *caudal* homolog *pal-1*. Although some aspects of the *unc-62* and *nob-1* Nob phenotypes are similar, others are not. For example, we did not detect posterior to anterior cell fate transformations in the E lineage of *unc-62(s472)* embryos, and the severe enclosure defects and hypodermal cell disorganization in these embryos are more similar to *pal-1* than to *nob-1* Nobs [see Fig. 4 and supplemental Fig. S2 and Fig. S5 (http://dev.biologists.org/ supplemental/)]. In experiments with a rescuing *nob-1::GFP* reporter construct, the number of *nob-1*-expressing cells was not significantly altered in *unc-62(RNAi)* embryos, and overexpression of *nob-1* did not rescue the *unc-62* phenotype (E. Kress and T. S., unpublished). Furthermore, presence of the *unc-62(e644)* allele did not increase the lethality resulting from a weak *nob-1* allele (E. Kress and T. S., unpublished). We conclude that there is so far no convincing evidence for an essential co-factor role, and that the *unc-62* phenotypes are not primarily the result of altered NOB-1 function. We have not tested for possible interactions of *unc-62* products with the later acting Hox gene functions of *lin-39, mab-5* and *egl-5*. Possible interactions of *unc-62* and *pal-1* functions are under investigation.

Table 4. Comparison of Nob embryonic phenotypes resulting from strong lf alleles of *unc-62*, *pal-1* and *nob-1

Phenotype	Defective gene		
	unc-62†	*pal-1*‡	*nob-1*§
Misplaced hypodermal precursors, early embryo	+	+	–
Misplaced hypodermal precursors, late embryo	+	+	±¶
Enclosure defects, ventral cleft	+	+	–
Enclosure defects, ventral hypodermis	+	+	±¶
P→A lineage transformations	–	–	+

*Based on results in this paper, previously published work (Edgar et al., 2001; Van Auken et al., 2000; Van Auken, 1998) and unpublished results.

†Homozygous mutant progeny embryos of *s472/+* heterozygous hermaphrodites or progeny embryos of *t2012* homozygous hermaphrodites.

‡Homozygous mutant progeny embryos of *pal-1(ct224)/+* heterozygous hermaphrodites; early *pal-1* functions (Hunter and Kenyon, 1996) are maternally supplied (Edgar et al., 2001).

§These strong *lf* alleles are deletions that probably eliminate function of both *nob-1* and *php-3*, whose functional relationships are not yet clear (Van Auken et al., 2000).

¶These phenotypes are less severe than in *unc-62(lf)* and *pal-1(lf)* embryos (see text).

Are UNC-62 proteins required to mediate nuclear localization of CEH-20, as might be expected from findings in other organisms? It appears that this requirement may be partial rather than complete; *unc-62*-defective embryos show variable nuclear localization of a translational CEH-20::GFP reporter in CEH-20-expressing cells, with less localization in early than in late embryos [see supplemental Fig. S4 (http://dev.biologists.org/supplemental/)], as if other mechanisms of CEH-20 nuclear import may exist.

Although the identity and interactions of all the players are not yet clear, our results do suggest that embryonically acting *unc-62* products are involved in controlling hypodermal specification, differentiation and morphogenesis. In wild-type embryos, dorsal and lateral hypodermal cell precursors form distinct populations that reside next to each other initially on the dorsal side of the embryo. We observed early *s472*, *t2012* and *ct344* mutant embryos in which dorsal and lateral hypodermal precursors intermingled, and fewer than the normal number of cells expressing hypodermal markers formed subsequently. These abnormalities probably contribute to later morphological defects, as successful enclosure, elongation and morphogenesis require proper hypodermal cell arrangement and function (Priess and Hirsh, 1986; Williams-Masson et al., 1998; Williams-Masson et al., 1997). The abnormal mixing of hypodermal cell populations in these mutants may indicate involvement of *unc-62* in maintaining distinct hypodermal cell identities, perhaps similar to the role of *Drosophila hth* in specifying distinct populations of cells that normally do not intermingle in the leg (Wu and Cohen, 1999) and eye-antenna (Pichaud and Casares, 2000) imaginal discs.

There are several differences between *C. elegans* and *Drosophila* that may somehow be related to our finding that phenotypes caused by *unc-62*, *ceh-20* and *ceh-40* mutations are not as expected from observations on the homologous *Drosophila* genes. Whereas in *Drosophila* only one PBC-family and one MEIS-family gene have been reported, *C. elegans* has at least two PBC-family genes. Furthermore, the *unc-62* gene generates four different transcripts by alternative

splicing, while *Drosophila hth* transcripts are not alternatively spliced. Therefore, *C. elegans*, with several PBC-family and Meis-family proteins, resembles vertebrates more closely than *Drosophila* with regard to the repertoire and possible interactions of these cofactors. A second possibly relevant difference between *C. elegans* and *Drosophila* could be that *C. elegans* requires only anterior-group and posterior-group Hox gene functions for embryonic survival (Brunschwig et al., 1999; Van Auken et al., 2000). As PBC- and Meis-family proteins can act as cofactors for Hox proteins, the fact that medial-group Hox proteins are essential for completion of embryogenesis in *Drosophila* but not *C. elegans* might account for different phenotypes resulting from loss of co-factor functions.

We are grateful to D. Baillie, R. Schnabel and A. Chisholm for *unc-62* alleles; to M. Stern for *ceh-20* alleles and unpublished results; to H. Kagoshima and T. Burglin for the *ceh-20::GFP* construct; to Y. Kohara for cDNAs; to Yo Suzuki and Dan Escovitz for assistance with several experiments; and to J. Yoder for the wild-type image in Fig. 6A. We thank M. Han, in whose laboratory the *ku234* allele was isolated, for support and encouragement; Andrew Taft and Chris Link for assistance with the QPCR experiments; and Lucie Yang and Cynthia Kenyon for pointing out to us the molecular lesion in *ku234*. We also thank the Genome Sequencing Center, Washington University, St Louis for communication of DNA sequence data prior to publication. Some strains were obtained from the Caenorhabditis Genetics Center, which is supported by the NIH Division of Research Resources. This research was supported by grants to W. B. W. (HD-14958) and M. S. (GM-58540) from NIH.

REFERENCES

Abu-Shaar, M., Ryoo, H. D. and Mann, R. S. (1999). Control of the nuclear localization of Extradenticle by competing nuclear import and export signals. *Genes Dev.* **13**, 935-945.

Affolter, M., Marty, T. and Vigano, M. A. (1999). Balancing import and export in development. *Genes Dev.* **13**, 913-915.

Babu, P. (1974). Biochemical genetics of *Caenorhabditis elegans*. *Mol. Gen. Genet.* **135**, 39-44.

Beanan, M. J. and Strome, S. (1992). Characterization of a germ-line proliferation mutation in *C. elegans*. *Development* **116**, 755-766.

Berthelsen, J., Kilstrup-Nielsen, C., Blasi, F., Mavilio, F. and Zappavigna, V. (1999). The subcellular localization of PBX1 and EXD proteins depends on nuclear import and export signals and is modulated by association with PREP1 and HTH. *Genes Dev.* **13**, 946-953.

Brenner, S. (1974). The genetics of *Caenorhabditis elegans*. *Genetics* **77**, 71-94.

Brunschwig, K., Wittmann, C., Schnabel, R., Burglin, T. R., Tobler, H. and Mueller, F. (1999). Anterior organization of the *Caenorhabditis elegans* embryo by the labial-like Hox gene *ceh-13*. *Development* **126**, 1537-1546.

Burglin, T. R. (1997). Analysis of TALE superclass homeobox genes (MEIS, PBC, KNOX, Iroquois, TGIF) reveals a novel domain conserved between plants and animals. *Nucleic Acids Res.* **25**, 4173-4180.

Chan, S., Jaffe, L., Capovilla, M., Botas, J. and Mann, R. (1994). The DNA binding specificity of ultrabithorax is modulated by cooperative interactions with extradenticle, another homeoprotein. *Cell* **78**, 603-615.

Chisholm, A. (1991). Control of cell fate in the tail region of *C. elegans* by the gene *egl-5*. *Development* **111**, 921-932.

Clark, S., Chisholm, A. and Horvitz, H. (1993). Control of cell fates in the central body region of *C. elegans* by the homeobox gene *lin-39*. *Cell* **74**, 43-55.

Edgar, L. G., Carr, S., Wang, H. and Wood, W. B. (2001). Zygotic expression of the *caudal* homolog *pal-1* is required for posterior patterning in *Caenorhabditis elegans* embryogenesis. *Dev. Biol.* **229**, 71-88.

Ekker, S. C., Jackson, D. G., von Kessler, D. P., Sun, B. I., Young, K. E. and Beachy, P. A. (1994). The degree of variation in DNA sequence recognition among four Drosophila homeotic proteins. *EMBO J.* **13**, 3551-3560.

Giulietti, A., Overbergh, L., Valckx, D., Decallonne, B., Bouillon, R. and Mathieu, C. (2001). An overview of real-time quantitative PCR: applications to quantify cytokine gene expression. *Methods* **25**, 386-401.

Hoey, T. and Levine, M. (1988). Divergent homeo box proteins recognize similar DNA sequences in Drosophila. *Nature* **332**, 858-861.

Kimble, J., Edgar, L. and Hirsh, D. (1984). Specification of male development in *Caenorhabditis elegans*: the *fem* genes. *Dev. Biol.* **105**, 234-239.

Kurant, E., Eytan, D. and Salzberg, A. (2001). Mutational analysis of the Drosophila *homothorax* gene. *Genetics* **157**, 689-698.

Labouesse, M., Hartwieg, E. and Horvitz, H. R. (1996). The *Caenorhabditis elegans* LIN-26 protein is required to specify and/or maintain all non-neuronal ectodermal cell fates. *Development* **122**, 2579-2588.

Lipardi, C., Wei, Q. and Paterson, B. M. (2001). RNAi as random degradative PCR. siRNA primers convert mRNA into dsRNAs that are degraded to generate new siRNAs. *Cell* **107**, 297-307.

Liu, J. and Fire, A. (2000). Overlapping roles of two Hox genes and the exd ortholog *ceh-20* in diversification of the *C. elegans* postembryonic mesoderm. *Development* **127**, 5179-5190.

Livak, K. J. and Schmittgen, T. D. (2001). Analysis of relative gene expression data using real-time quantitative PCR and the 2(–Delta Delta C(T)) method. *Methods* **25**, 402-408.

Manak, J. and Scott, M. (1994). A class act: conservation of homeodomain protein functions. *Development* **Suppl.**, 61-71.

Mann, R. S. (1995). The specificity of homeotic gene function. *BioEssays* **17**, 855-863.

Mann, R. S. and Affolter, M. (1998). *Hox* proteins meet more partners. *Curr. Opin. Genet. Dev.* **8**, 423-429.

Mann, R. S. and Chan, S. K. (1996). Extra specificity from *extradenticle*: the partnership between HOX and PBX/EXD homeodomain proteins. *Trends Genet.* **12**, 258-262.

Montgomery, M. K., Xu, S. and Fire, A. (1998). RNA as a target of double-stranded RNA-mediated genetic interference in *Caenorhabditis elegans*. *Proc. Natl. Acad. Sci. USA* **95**, 15502-15507.

Pai, C. Y., Kuo, T. S., Jaw, T. J., Kurant, E., Chen, C. T., Bessarab, D. A., Salzberg, A. and Sun, Y. H. (1998). The Homothorax homeoprotein activates the nuclear localization of another homeoprotein, extradenticle, and suppresses eye development in Drosophila. *Genes Dev.* **12**, 435-446.

Pichaud, F. and Casares, F. (2000). *homothorax* and *iroquois-C* genes are required for the establishment of territories within the developing eye disc. *Mech. Dev.* **96**, 15-25.

Priess, J. R. and Hirsh, D. I. (1986). *Caenorhabditis elegans* morphogenesis: The role of the cytoskeleton in elongation of the embryo. *Dev. Biol.* **117**, 156-173.

Pulak, R. and Anderson, P. (1993). mRNA surveillance by the *Caenorhabditis elegans smg* genes. *Genes Dev.* **7**, 1885-1897.

Rieckhof, G. E., Casares, F., Ryoo, H. D., Abu-Shaar, M. and Mann, R. S. (1997). Nuclear translocation of Extradenticle requires Homothorax, which encodes an Extradenticle-related homeodomain protein. *Cell* **91**, 171-183.

Rosenbluth, R., Rogalski, T., Johnson, R., Addison, L. and Baillie, D. (1988). Genomic organization in *Caenorhabditis elegans*: deficiency mapping on linkage group V(left). *Genet. Res.* **52**, 105-118.

Ryoo, H. D., Marty, T., Casares, F., Affolter, M. and Mann, R. S. (1999). Regulation of Hox target genes by a DNA bound Homothorax/Hox/Extradenticle complex. *Development* **126**, 5137-5148.

Schauer, I. and Wood, W. (1990). Early *C. elegans* embryos are transcriptionally active. *Development* **110**, 1303-1317.

Shen, W. F., Montgomery, J. C., Rozenfeld, S., Moskow, J. J., Lawrence, H. J., Buchberg, A. M. and Largman, C. (1997a). AbdB-like Hox proteins stabilize DNA binding by the Meis1 homeodomain proteins. *Mol. Cell. Biol.* **17**, 6448-6458.

Shen, W. F., Rozenfeld, S., Lawrence, H. J. and Largman, C. (1997b). The Abd-B-like Hox homeodomain proteins can be subdivided by the ability to form complexes with Pbx1a on a novel DNA target. *J. Biol. Chem.* **272**, 8198-8206.

Siddiqui, S. (1990). Mutations affecting axonal growth and guidance of motor neurons and mechanosensory neurons in the nematode Caenorhabditis elegans. *Neurosci. Res.* **13**, 171-190.

Streit, A., Li, W., Robertson, B., Schein, J., Kamal, I. H., Marra, M. and

Wood, W. B. (1999). Homologs of the *Caenorhabditis elegans* masculinizing gene *her-1* in *C. briggsae* and the filarial parasite *Brugia malayi*. *Genetics* **152**, 1573-1584.

Sulston, J. and Hodgkin, J. (1988). Methods. In *The Nematode* Caenorhabditis elegans (ed. W. B. Wood), pp. 81-122. Cold Spring Harbor, NY: Cold Spring Harbor Laboratory Press.

Tabara, H., Grishok, A. and Mello, C. C. (1998). RNAi in *C. elegans*: soaking in the genome sequence. *Science* **282**, 430-431.

Takacs-Vellai, K., Vellai, T., Vigano, A., Affolter, M. and Mueller, F. (2002). A functional analysis of the *extradenticle* ortholog *ceh-40*. *Abstracts, European C. elegans meeting, Paestum, Italy, May 18-21.*, 197.

Thomas, C., DeVries, P., Hardin, J. and White, J. (1996). Four-dimensional imaging: computer visualization of 3D movements in living specimens. *Science* **273**, 603-607.

Thomas, J., Stern, M. and Horvitz, H. (1990). Cell interactions coordinate the development of the *C. elegans* egg-laying system. *Cell* **62**, 1041-1052.

Trent, C., Tsung, N. and Horvitz, H. R. (1983). Egg-laying defective mutants of the nematode *Caenorhabditis elegans*. *Genetics* **104**, 619-647.

Van Auken, K., Weaver, D. C., Edgar, L. G. and Wood, W. B. (2000). *C. elegans* embryonic axial patterning requires two recently discovered posterior-group Hox genes. *Proc. Natl. Acad. Sci. USA* **97**, 4499-4503.

Van Auken, K. M. (1998). Genetic and molecular analysis of *nob-1*, a gene required for posterior development in the *Caenorhabditis elegans* embryo. PhD dissertation, University of Colorado, Boulder, CO.

van Dijk, M. and Murre, C. (1994). Extradenticle raises the Dna binding specificity of homeotic selector gene products. *Cell* **78**, 617-624.

Wang, B., Muller-Immergluck, M., Austin, J., Robinson, N., Chisholm, A. and Kenyon, C. (1993). A homeotic gene cluster patterns the anteroposterior body axis of *C. elegans*. *Cell* **74**, 29-42.

Williams-Masson, E. M., Heid, P. J., Lavin, C. A. and Hardin, J. (1998). The cellular mechanism of epithelial rearrangement during morphogenesis of the *Caenorhabditis elegans* dorsal hypodermis. *Dev. Biol.* **204**, 263-276.

Williams-Masson, E. M., Malik, A. N. and Hardin, J. (1997). An actin-mediated two-step mechanism is required for ventral enclosure of the *C. elegans* hypodermis. *Development* **124**, 2889-2901.

Wrischnik, L. A. and Kenyon, C. J. (1997). The role of *lin-22*, a *hairy/enhancer of split* homolog, in patterning the peripheral nervous system of *C. elegans*. *Development* **124**, 2875-2888.

Wu, J. and Cohen, S. M. (1999). Proximodistal axis formation in the Drosophila leg: subdivision into proximal and distal domains by Homothorax and Distal-less. *Development* **126**, 109-117.